Journal of Computational Physics 227 (2008) 9711–9726

Contents lists available at ScienceDirect

Journal of Computational Physics

journal homepage: www.elsevier.com/locate/jcp

The effects of slope limiting on asymptotic-preserving numerical methods for hyperbolic conservation laws

Ryan G. McClarren *, Robert B. Lowrie

Computational Physics Group (CCS-2), Los Alamos National Laboratory[1], P.O. Box 1663, MS D413, Los Alamos, NM 87545, United States

ARTICLE INFO

Article history:
Received 8 November 2007
Received in revised form 10 July 2008
Accepted 13 July 2008
Available online 6 August 2008

Keywords:
Asymptotic-preserving numerical methods
Discontinuous Galerkin
Slope limiters
Thermal radiative transfer

ABSTRACT

Many hyperbolic systems of equations with stiff relaxation terms reduce to a parabolic description when relaxation dominates. An asymptotic-preserving numerical method is a discretization of the hyperbolic system that becomes a valid discretization of the parabolic system in the asymptotic limit. We explore the consequences of applying a slope limiter to the discontinuous Galerkin (DG) method, with linear elements, for hyperbolic systems with stiff relaxation terms. Without a limiter, the DG method gives an accurate discretization of the Chapman–Enskog approximation of the system when the relaxation length scale is not resolved. It is well known that the first-order upwind (or "step") method fails to obtain the proper asymptotic limit. We show that using the minmod slope limiter also fails, but that using double minmod gives the proper asymptotic limit. Despite its effectiveness in the asymptotic limit, the double minmod limiter allows artificial extrema at cell interfaces, referred to as "sawteeth". We present a limiter that eliminates the sawteeth, but maintains the proper asymptotic limit. The systems that we analyze are the hyperbolic heat equation and the P_n thermal radiation equations. Numerical examples are used to verify our analysis.

1. Introduction

There is a multiplicity of physical phenomena that are described by a hyperbolic system of conservation laws with stiff relaxation terms. Some examples are the radiation–hydrodynamics system [1,2], charge transport in semiconductors, and neutron transport in scattering media [3,4]. The Chapman–Enskog approximation [5] to these systems displays parabolic behavior to leading order [6]; this is often referred to as the asymptotic or diffusion limit.

Despite the fact that the underlying equations are parabolic in the asymptotic limit, there is no guarantee that a numerical method for the hyperbolic system will limit to a valid discretization of the asymptotic limit of the continuous equations. Methods that do limit to an accurate description in the asymptotic limit are said to be asymptotic preserving,[2] a term coined in Ref. [7]. Past work on such discretizations includes Refs. [6,8,9]. One type of method that has been shown to be asymptotic-preserving is the discontinuous Galerkin method with linear elements [1,10,11], which we will refer to throughout this study as simply the "DG method". However, these studies did not take into account the effect of a slope limiter on the ability of the method to preserve the asymptotic limit.

* Corresponding author. Tel.: +1 505 665 1397.
E-mail address: ryanmc@lanl.gov (R.G. McClarren).

[1] Los Alamos National Laboratory is operated by Los Alamos National Security, LLC for the US Department of Energy under Contract DE-AC52-06NA25396. LA-UR-07-7512.

[2] This terminology is not constant across discipline boundaries: in the radiation transport community an asymptotic-preserving method is said to have a valid diffusion limit.

0021-9991/$ - see front matter © 2008 Published by Elsevier Inc.
doi:10.1016/j.jcp.2008.07.012

Slope limiters are used to address the fact that second-order methods for hyperbolic problems must be nonlinear to avoid artificial oscillations in the solution. A slope limiter nonlinearly adapts the numerical method to suppress artificial oscillations. On the other hand, in the asymptotic limit of many systems, a slope limiter is not necessary because in that limit the system becomes a diffusion equation. Nevertheless, it is common to continue to use a slope limiter in such regions because it may be difficult to assess locally when the asymptotic regime applies. In other systems advection is present in the asymptotic limit and a limiter remains necessary. For example, radiation transport in a static medium asymptotically reduces to a parabolic equation in the small mean-free-path limit. A limiter is unnecessary in this limit. However, when radiation transport is coupled with hydrodynamic motion, advection terms may dominate in the asymptotic limit and a slope limiter is useful in all regimes.

It is known that the asymptotic-preserving quality of the DG method relies on the solution representation limiting to a continuous function in the asymptotic limit [12]. We demonstrate that certain slope limiters will introduce discontinuities at the cell edges. A consequence of breaking continuity can be the failure of the method to preserve the asymptotic limit. The conservation laws that we consider are the hyperbolic heat equation and the P_N equations of thermal radiation transport.

In the next section we begin by reviewing the DG method. We then apply the method to the hyperbolic heat equation and examine its properties in the limit of large relaxation terms. After showing that the DG method without a slope limiter preserves the asymptotic limit of the hyperbolic heat equation, we analyze the effects of a slope limiter in the asymptotic limit. In Section 5, we introduce a modification to the double minmod limiter that removes false extrema, but maintains the proper asymptotic behavior. Numerical results for the hyperbolic heat equation are presented in Section 6. We apply our analysis of the hyperbolic heat equation to the thermal radiation transport equations and present numerical results in Section 7. In Section 8, we present our conclusions from this study.

2. The discontinuous Galerkin method

In this section we review the discontinuous Galerkin method, with linear elements, for a hyperbolic system with source terms. Again, we refer to this method as simply the DG method. This method has been shown in the past to be asymptotic preserving without a slope limiter [1,12,13].

The general hyperbolic system that we will be analyzing can be written as

$$\frac{\partial u}{\partial t}+\frac{\partial}{\partial x}\mathbf{f}(\mathbf{u})=\mathbf{s}(\mathbf{u}), \tag{1}$$

where $\mathbf{u}$, $\mathbf{f}(\mathbf{u})$ and $\mathbf{s}(\mathbf{u})$ are vectors of length p. To apply the discontinuous Galerkin method to this system we impose a spatial mesh of cells, each on the interval $[x_{m-1/2},x_{m+1/2}]$ with $\Delta x_m = x_{m+1/2}-x_{m-1/2}$. We write the value of $\mathbf{u}$ in cell m as

$$\mathbf{u}_m(x,t)=\sum_{j=0}^{k}\mathbf{u}_{m,j}(t)B_j(x). \tag{2}$$

Here, $B_j(x)$ is a basis function on cell m and k is the number of basis functions. These bases are defined on a reference element where $x\in[x_{m-1/2},x_{m+1/2}]$ is mapped to $\xi\in[0,1]$. In this paper, we use linear elements so that

$$B_1(\xi)=1-\xi,\qquad B_2(\xi)=\xi. \tag{3}$$

We now multiply Eq. (1) by a basis function B_j, integrate over a cell, and integrate the advection term by parts. This results in

$$\Delta x\frac{\mathrm{d}}{\mathrm{d}t}\int_0^1 \mathrm{d}\xi B_j(\xi)\mathbf{u}+B_j(1)\mathbf{f}_{m+1/2}-B_j(0)\mathbf{f}_{m-1/2}-\int_0^1 \mathrm{d}\xi\mathbf{f}(\mathbf{u})\frac{\partial}{\partial\xi}B_j(\xi)=\Delta x\int_0^1 \mathrm{d}\xi B_j(\xi)\mathbf{s}(\mathbf{u}), \tag{4}$$

where now we drop the cell index subscript "m" unless needed. The interface flux is defined as

$$\mathbf{f}_{m+1/2}=F(\mathbf{u}_m(x_{m+1/2},t),\mathbf{u}_{m+1}(x_{m+1/2},t)), \tag{5}$$

where F is any suitable flux function.

When we replace $\mathbf{u}$ in Eq. (4) with the expansion (Eqs. (2) and (3)) and assume that both $\mathbf{f}(\mathbf{u})$ and $\mathbf{s}(\mathbf{u})$ also vary linearly over the cell, we obtain

$$\mathbf{M}\frac{\mathrm{d}}{\mathrm{d}t}\begin{pmatrix}\mathbf{u}_1\\ \mathbf{u}_2\end{pmatrix}+\frac{1}{2}\begin{pmatrix}\mathbf{f}_1+\mathbf{f}_2-2\mathbf{f}_{m-1/2}\\ \mathbf{f}_{m+1/2}-\mathbf{f}_1-\mathbf{f}_2\end{pmatrix}=\mathbf{M}\begin{pmatrix}\mathbf{s}_1\\ \mathbf{s}_2\end{pmatrix}, \tag{6}$$

where the mass matrix is given by

$$\mathbf{M}=\frac{\Delta x}{6}\begin{pmatrix}2&1\\1&2\end{pmatrix}. \tag{7}$$

Then multiply through by $\mathbf{M}^{-1}$ to obtain

$$\frac{\mathrm{d}}{\mathrm{d}t}\begin{pmatrix}\mathbf{u}_1\\ \mathbf{u}_2\end{pmatrix}+\frac{1}{\Delta x}\begin{pmatrix}-2\mathbf{f}_{m+1/2}-4\mathbf{f}_{m-1/2}+3(\mathbf{f}_1+\mathbf{f}_2)\\ 4\mathbf{f}_{m+1/2}+2\mathbf{f}_{m-1/2}-3(\mathbf{f}_1+\mathbf{f}_2)\end{pmatrix}=\begin{pmatrix}\mathbf{s}_1\\ \mathbf{s}_2\end{pmatrix}. \tag{8}$$

As in Ref. [1], we integrate Eq. (8) in time using a simple predictor–corrector approach. The predictor step is

$$\frac{\mathbf{U}^{n+1/2}-\mathbf{U}^{n}}{\Delta t/2}+\mathbf{F}^{n}=\mathbf{S}^{n+1/2}, \tag{9}$$

where the superscript n represents the nth time level, and

$$\mathbf{U}=\begin{pmatrix}\mathbf{u}_1\\ \mathbf{u}_2\end{pmatrix},\quad \mathbf{F}=\frac{1}{\Delta x}\begin{pmatrix}-2\mathbf{f}_{m+1/2}-4\mathbf{f}_{m-1/2}+3(\mathbf{f}_1+\mathbf{f}_2)\\ 4\mathbf{f}_{m+1/2}+2\mathbf{f}_{m-1/2}-3(\mathbf{f}_1+\mathbf{f}_2)\end{pmatrix},\quad \mathbf{S}=\begin{pmatrix}\mathbf{s}_1\\ \mathbf{s}_2\end{pmatrix}. \tag{10}$$

The corrector step is

$$\frac{\mathbf{U}^{n+1}-\mathbf{U}^{n}}{\Delta t}+\mathbf{F}^{n+1/2}=\mathbf{S}^{n+1}. \tag{11}$$

This time integrator is equivalent to second-order Runge–Kutta for the advection terms and backward Euler for the source term.

Note that our treatment is semi-implicit: the advection is treated explicitly and the relaxation is implicitly integrated. The method is stable without resolving the relaxation time scale. However, the explicit treatment of the advection terms results in a time step limit based on the Courant number for the maximum absolute advection speed. The maximum allowable Courant number is 1/3 [14]. The overall method is locally implicit in the sense that $\mathbf{U}_{m,j}$ is not implicitly coupled to values at other m- and j-indices.

3. The hyperbolic heat equation

To show the properties of the DG method we will first examine the hyperbolic heat equation, a simple system of conservation laws that limits to a parabolic description in the asymptotic limit. The analysis of this system will show why the DG method works in the asymptotic limit and how slope limiters can cause it to fail.

The hyperbolic heat equation is a 2×2 system in the form of Eq. (1) given by

$$\frac{\partial u}{\partial t}+\frac{\partial v}{\partial x}=0, \tag{12}$$

$$\frac{\partial v}{\partial t}+\frac{\partial u}{\partial x}=-\frac{v}{\tau}, \tag{13}$$

where $\tau\geqslant 0$. The long time behavior of this system away from boundaries can be determined using the following scaling:

$$\frac{\partial u}{\partial t}+\frac{1}{\epsilon}\frac{\partial v}{\partial x}=0, \tag{14}$$

$$\frac{\partial v}{\partial t}+\frac{1}{\epsilon}\frac{\partial u}{\partial x}=-\frac{v}{\tau\epsilon^2}, \tag{15}$$

with $\epsilon>0$. When ϵ is small, u is governed to leading order in ϵ by the heat equation [6,13]

$$\frac{\partial u}{\partial t}=\tau\frac{\partial^2 u}{\partial x^2} \tag{16}$$

and, to leading order in ϵ, v takes the form of a Fick's law:

$$v=-\tau\frac{\partial u}{\partial x}. \tag{17}$$

The DG method (8) for this system takes

$$\mathbf{u}=\begin{pmatrix}u\\ v\end{pmatrix},\qquad \mathbf{f}=\frac{1}{\epsilon}\begin{pmatrix}v\\ u\end{pmatrix},\qquad \mathbf{s}=-\frac{1}{\tau\epsilon^2}\begin{pmatrix}0\\ v\end{pmatrix}. \tag{18}$$

We use the interface flux

$$\mathbf{f}_{m+1/2}=\frac{1}{2\epsilon}\begin{pmatrix}0&1\\ 1&0\end{pmatrix}\begin{pmatrix}u_{m,2}+u_{m+1,1}\\ v_{m,2}+v_{m+1,1}\end{pmatrix}-\frac{1}{2\epsilon}\begin{pmatrix}1&0\\ 0&1\end{pmatrix}\begin{pmatrix}u_{m+1,1}-u_{m,2}\\ v_{m+1,1}-v_{m,2}\end{pmatrix}. \tag{19}$$

This is the "frozen" upwind flux [2] based on an eigenfunction decomposition of the system ignoring the relaxation terms.

3.1. Asymptotic limit of DG method for the hyperbolic heat equation

We will now show that the DG method for the hyperbolic heat equation will give a valid discretization of Eqs. (16) and (17) in the limit of small τ and away from boundaries and initial layers. The analysis in this section complements that of

Lowrie and Morel [13], who used a modified-equation analysis and lumped the mass matrix. Larsen et al. [8] have also shown that the DG method has the proper asymptotic limit for linear transport.

We can quantify the resolution of small scales with the parameter h:

$$h = \frac{\Delta x}{\tau}, \tag{20}$$

where Δx is the mesh spacing (in previous work h has been called the numerical Peclet number [6]). We will be concerned with the case where the $h \gg 1$. This case, also called the unresolved regime, implies that the numerical grid does not resolve the relaxation scale. In the radiation transport community the analogous case is said to have optically thick cells, meaning Δx is much greater than a mean free path for radiation. The unresolved regime has the relaxation term v/τ dominating the advection terms. In this regime, we desire a numerical method to solve to leading order the asymptotic limit of the original equations. Such a method is said to be asymptotic preserving. For the hyperbolic heat equations we would like our method to approximate the heat equation in the case of $h \gg 1$.

The semi-discrete DG method (6) may be written for each unknown as

$$\mathbf{M}\frac{\mathrm{d}}{\mathrm{d}t}\begin{pmatrix} u_1 \\ u_2 \end{pmatrix} + \frac{1}{2\epsilon}\begin{pmatrix} v_{m,2} - v_{m-1,2} + u_{m,1} - u_{m-1,2} \\ v_{m+1,1} - v_{m,1} + u_{m,2} - u_{m+1,1} \end{pmatrix} = 0 \tag{21}$$

and

$$\mathbf{M}\frac{\mathrm{d}}{\mathrm{d}t}\begin{pmatrix} v_1 \\ v_2 \end{pmatrix} + \frac{1}{2\epsilon}\begin{pmatrix} u_{m,2} - u_{m-1,2} + v_{m,1} - v_{m-1,2} \\ u_{m+1,1} - u_{m,1} + v_{m,2} - v_{m+1,1} \end{pmatrix} = -\frac{1}{\tau\epsilon^2}\mathbf{M}\begin{pmatrix} v_1 \\ v_2 \end{pmatrix}. \tag{22}$$

To proceed we assume a regular expansion of u and v in ϵ:

$$(\cdot) = \sum_{j=0}^{\infty} \epsilon^j (\cdot)^{(j)}. \tag{23}$$

By equating terms of equal order in ϵ, Eq. (22) gives that

$$v_{m,1}^{(0)} = v_{m,2}^{(0)} = 0. \tag{24}$$

Using this result, Eq. (21) gives

$$u_{m+1,1}^{(0)} = u_{m,2}^{(0)} \equiv u_{m+1/2}^{(0)}. \tag{25}$$

In other words, $u^{(0)}$ is continuous, with the value $u_{m+1/2}^{(0)}$ defined as the leading-order solution at the node location $x_{m+1/2}$. The continuity of the leading-order solution is referred to as a solvability condition in Ref. [12].

The O(ϵ) terms of Eq. (22) are

$$\frac{1}{2}(u_{m+1/2}^{(0)} - u_{m-1/2}^{(0)})\begin{pmatrix} 1 \\ 1 \end{pmatrix} = -\frac{1}{\tau}\mathbf{M}\begin{pmatrix} v_{m,1}^{(1)} \\ v_{m,2}^{(1)} \end{pmatrix}, \tag{26}$$

where we have used Eq. (25). Consequently,

$$v_{m,1}^{(1)} = v_{m,2}^{(1)} = -\tau\frac{u_{m+1/2}^{(0)} - u_{m-1/2}^{(0)}}{\Delta x} \equiv v_m^{(1)}, \tag{27}$$

so that $v^{(1)}$ is constant in each cell m, with the value denoted as $v_m^{(1)}$.

The O(ϵ) terms of Eq. (21) are

$$\frac{\Delta x}{6}\frac{\mathrm{d}}{\mathrm{d}t}\begin{pmatrix} 2u_{m-1/2}^{(0)} + u_{m+1/2}^{(0)} \\ 2u_{m+1/2}^{(0)} + u_{m-1/2}^{(0)} \end{pmatrix} + \frac{1}{2}\begin{pmatrix} v_m^{(1)} - v_{m-1}^{(1)} + u_{m,1}^{(1)} - u_{m-1,2}^{(1)} \\ v_{m+1}^{(1)} - v_m^{(1)} + u_{m,2}^{(1)} - u_{m+1,1}^{(1)} \end{pmatrix} = 0, \tag{28}$$

where we have used Eqs. (25) and (27). If we substitute $m \to m+1$ in the first equation, add it to the second, and use Eq. (27), we obtain

$$\frac{1}{6}\frac{d}{dt}(u_{m+3/2}^{(0)} + 4u_{m+1/2}^{(0)} + u_{m-1/2}^{(0)}) = \tau\frac{u_{m+3/2}^{(0)} - 2u_{m+1/2}^{(0)} + u_{m-1/2}^{(0)}}{\Delta x^2}. \tag{29}$$

This is a valid spatial discretization of the heat equation, Eq. (16); indeed, it is the continuous, piecewise linear finite-element discretization of Eq. (16), which is second-order accurate in space.

4. Slope limiting

To avoid the creation of artificial oscillations in the solution, it is commonplace to use a slope limiter with the DG method.[3] Slope limiters are typically not needed for DG in the asymptotic limit if the leading-order equations have no advection terms. If advection terms are present in the asymptotic limit, then slope limiting is very useful in order to suppress artificial oscillations. Even for systems that lack advection terms in the asymptotic limit, in many applications, it is not known *a priori* locations where the asymptotic limit holds. In these problems a slope limiter, or some sort of "flux fix-up", would likely be applied throughout the domain. These reasons motivate our analysis of the effect of a slope limiting in the asymptotic limit.

The slope limiting process we follow is similar to that in Ref. [15]. After each predictor or corrector step, the average value in each cell is computed:

$$\bar{\mathbf{u}}_m = \frac{1}{2}(\mathbf{u}_{m,2} + \mathbf{u}_{m,1}). \tag{30}$$

We then adjust the node values to be bounded by the neighboring cell averages:

$$\tilde{\mathbf{u}}_{m,1} = \bar{\mathbf{u}}_m - \frac{\mathbf{s}_m}{2}, \tag{31}$$

$$\tilde{\mathbf{u}}_{m,2} = \bar{\mathbf{u}}_m + \frac{\mathbf{s}_m}{2}. \tag{32}$$

The slope in these equations is calculated, for each variable, using the formula

$$s_m = \text{minmod}(u_{m,2} - u_{m,1}, \alpha(\bar{u}_m - \bar{u}_{m-1}), \alpha(\bar{u}_{m+1} - \bar{u}_m)), \tag{33}$$

with $\alpha \in [0,2]$, and

$$\text{minmod}(a,b,c) = \begin{cases} \min(|a|,|b|,|c|) & \text{if } \text{sign}(a) = \text{sign}(b) = \text{sign}(c), \\ 0 & \text{otherwise.} \end{cases} \tag{34}$$

Different values of α give common slope limiters. When $\alpha = 0$ we recover the first-order Godunov scheme. In the transport literature, this method is referred to as the "step" method. With $\alpha = 1$ we recover the minmod limiter, and for $\alpha = 2$ we obtain the double minmod [16] (or monotonized-central or TVD minmod [15]) limiter. The slope limiters described above are linear once Eq. (34) is evaluated, a fact that has been taken advantage of in developing implicit methods for finite volume schemes [17]. We will now show how the effects of the slope limiter can change the method's behavior in the asymptotic limit.

4.1. Asymptotics of slope limited method

To analyze the slope limiter in the asymptotic regime we must make some assumptions about the shape of the solution in order to evaluate Eq. (34) and remove the nonlinearities of the slope limiter. To begin with, we postulate that the solution in the region of interest is a monotonic, increasing function of x. The case of a decreasing function follows trivially.

4.1.1. Step method

If we set $\alpha = 0$, the DG method reduces to the step method. In this case we have

$$\mathbf{u}_{m,1} = \mathbf{u}_{m,2} = \bar{\mathbf{u}}_m. \tag{35}$$

For transport, the step method has already been shown not to preserve the asymptotic solution [8], so we expect the same result here.

The solvability condition that gave us the continuity of $u^{(0)}$, Eq. (25), in this case becomes

$$\bar{u}^{(0)}_{m+1} = \bar{u}^{(0)}_m. \tag{36}$$

In other words, the step method gives a leading-order solution that is a constant. Continuing with the asymptotic analysis, Eq. (27) then gives $\tilde{v}^{(1)} = 0$ and the "diffusion" equation we get is

$$\frac{1}{6}\frac{\mathrm{d}}{\mathrm{d}t}(u^{(0)}_{m+3/2} + 4u^{(0)}_{m+1/2} + u^{(0)}_{m-1/2}) = 0. \tag{37}$$

This is clearly not the correct asymptotic limit: the leading-order solution is constant and the leading-order evolution equation is not a valid discretization of Eq. (16).

4.1.2. Minmod limiter

To begin our analysis, consider the difference

[3] It is possible to damp oscillations by lumping the mass matrix of the finite element equations, which adds numerical dissipation. However, lumping does not eliminate all oscillations because the resulting method remains second order and linear.

$$(\bar{u}_{m+1} - \bar{u}_m) - (u_{m,2} - u_{m,1}) = \frac{1}{2}u_{m+1,2} - u_{m,2} + \frac{1}{2}u_{m,1}, \tag{38}$$

the sign of which determines which slope the minmod limiter selects for cell m.

Assuming a smooth solution, we Taylor expand about $x = x_m + \Delta x/2$ to get

$$u_{m+1,2} = u_{m,2} + \Delta x\frac{\partial u}{\partial x} + \frac{\Delta x^2}{2}\frac{\partial^2 u}{\partial x^2} + \mathrm{O}(\Delta x^3),$$
$$u_{m,1} = u_{m,2} - \Delta x\frac{\partial u}{\partial x} + \frac{\Delta x^2}{2}\frac{\partial^2 u}{\partial x^2} + \mathrm{O}(\Delta x^3).$$

Substitute these expansions into Eq. (38) to obtain

$$(\bar{u}_{m+1} - \bar{u}_m) - (u_{m,2} - u_{m,1}) = \frac{\Delta x^2}{2}\frac{\partial^2 u}{\partial x^2} + \mathrm{O}(\Delta x^3). \tag{39}$$

Similarly,

$$(u_{m,2} - u_{m,1}) - (\bar{u}_m - \bar{u}_{m-1}) = \frac{\Delta x^2}{2}\frac{\partial^2 u}{\partial x^2} + \mathrm{O}(\Delta x^3). \tag{40}$$

Hence, for smooth data, the manner which minmod modifies the slope depends entirely on the second derivative of the solution.

First we will look at the case of the second derivative being positive. If the second derivative is positive, then the cell-average slope to the left of the cell is the smallest. The minmod slope for cell m is then

$$\tilde{s}_m = \frac{1}{2}(u_{m,2} + u_{m,1} - u_{m-1,2} - u_{m-1,1}) = \frac{1}{2}(u_{m,2} - u_{m-1,1}). \tag{41}$$

Using this slope the limited nodal values are

$$\tilde{u}_{m,1} = \frac{1}{2}u_{m,1} + \frac{1}{4}u_{m,2} + \frac{1}{4}u_{m-1,1}, \tag{42}$$
$$\tilde{u}_{m,2} = \frac{1}{2}u_{m,1} + \frac{3}{4}u_{m,2} - \frac{1}{4}u_{m-1,1}. \tag{43}$$

Consequently, the jump at the cell interface is given by

$$\tilde{u}_{m+1,1} - \tilde{u}_{m,2} = \frac{1}{4}(u_{m+1,2} - u_{m,2} - u_{m,1} + u_{m-1,1}). \tag{44}$$

Therefore, the minmod limiter does not maintain a continuous solution if the solution has a positive second derivative. Specifically, using Eq. (44), the leading-order solution replaces Eq. (25) with

$$\tilde{u}^{(0)}_{m+1,1} = \tilde{u}^{(0)}_{m,2} \equiv \tilde{u}^{(0)}_{m+1/2}. \tag{45}$$

Using the definitions of the minmod limited values in Eq. (45) leads to

$$u^{(0)}_{m+1,2} - u^{(0)}_{m,2} - u^{(0)}_{m,1} + u^{(0)}_{m-1,1} = 0. \tag{46}$$

For a smooth solution, this equation gives that

$$\frac{\partial^2 u^{(0)}}{\partial x^2} = \mathrm{O}(\Delta x). \tag{47}$$

Hence, the minmod limiter will force the second derivative of the solution to be order Δx (and, therefore, the solution approximately linear) when the relaxation terms are not resolved.

To get the minmod version of Eq. (29) we will use the identity

$$2\tilde{u}_{m+1/2} = \tilde{u}_{m,2} + \tilde{u}_{m+1,1}. \tag{48}$$

Substituting this into the limited version of Eq. (29) leads to

$$\frac{1}{6}\frac{\mathrm{d}}{\mathrm{d}t}(u^{(0)}_{m+3/2} + 4u^{(0)}_{m+1/2} + u^{(0)}_{m-1/2}) = \tau\frac{u^{(0)}_{m+1,2} - u^{(0)}_{m,2} - u^{(0)}_{m,1} + u^{(0)}_{m-1,1}}{\Delta x^2}. \tag{49}$$

The difference on the RHS of Eq. (49) is exactly the condition in Eq. (46). Therefore, the leading-order evolution equation is

$$\frac{1}{6}\frac{\mathrm{d}}{\mathrm{d}t}(u^{(0)}_{m+3/2} + 4u^{(0)}_{m+1/2} + u^{(0)}_{m-1/2}) = 0. \tag{50}$$

This is not a valid asymptotic limit. While for the minmod case the evolution equation is the same as in the step limiter, the minmod limiter will support a linear variation inside each cell whereas the step limiter makes the solution constant in each cell. Given this fact we would expect the minmod limiter to give smaller errors than the step limiter.

Although the above analysis assumed that the second derivative of u is positive, if we assume the second derivative of u is negative, then the slope to the right of cell m is used and the same result as Eq. (50) is obtained.

4.1.3. Double minmod

Previously, it was shown by Cockburn and Shu that the double minmod limiter will not effect smooth solutions away from extreme points [15]. Here, we briefly reprise an analysis that shows how this property allows the limiter to preserve the asymptotic limit.

In the case of the double minmod limiter we will follow the same procedure as for the minmod limiter, except there will be a factor of two multiplying the differences between cell averages. The double minmod version of Eq. (38) is

$$(u_{m,2} - u_{m,1}) - 2(\bar{u}_{m+1} - \bar{u}_m) = -\Delta x \frac{\partial u}{\partial x} + \mathrm{O}(\Delta x^2). \tag{51}$$

This implies that $u_{m,2} - u_{m,1} < 2(\bar{u}_{m+1} - \bar{u}_m)$ because Eq. (51) is negative for any positive Δx and we assumed from the outset that the solution was increasing. We now compare $u_{m,2} - u_{m,1}$ and $2(\bar{u}_m - \bar{u}_{m-1})$:

$$(u_{m,2} - u_{m,1}) - (\bar{u}_m - \bar{u}_{m-1}) = -\Delta x \frac{\partial u}{\partial x} + \mathrm{O}(\Delta x^2). \tag{52}$$

This result is also negative for any Δx implying that the slope, s_m is

$$s_m = u_{m,2} - u_{m,1}. \tag{53}$$

That is to say that node values will be unchanged by the double minmod limiter in this case of a smooth, monotonic function. The double minmod limiter does not change Eq. (25), allowing the rest of the asymptotic analysis to be valid and preserving the asymptotic limit of the hyperbolic heat equation.

The analysis above applies when the solution is monotone, but not at an extremum in the solution. For the remainder of this section, we will show that for an isolated extremum, a valid diffusion limit is obtained. To begin, it is straightforward to show that with no limiter, Eq. (29) implies that the leading-order, cell-average values satisfy a similar form:

$$\frac{1}{6}\frac{\mathrm{d}}{\mathrm{d}t}(\bar{u}^{(0)}_{m+1} + 4\bar{u}^{(0)}_m + \bar{u}^{(0)}_{m-1}) = \tau \frac{\bar{u}^{(0)}_{m+1} - 2\bar{u}^{(0)}_m + \bar{u}^{(0)}_{m-1}}{\Delta x^2}. \tag{54}$$

Again, this is a second-order accurate discretization of the heat equation.

Consider an isolated extremum within a cell with index m. Any limiter of the form (33) will zero the slope in cells whose cell-average value is a local extremum, so that

$$u^{(0)}_{m,1} = u^{(0)}_{m,2} \equiv \bar{u}^{(0)}_m. \tag{55}$$

Using the solvability condition, Eq. (25), the leading-order numerical solution at the node locations $m \pm 1/2$ is continuous. The double minmod limiter does not break this continuity. Therefore, the value $\bar{u}^{(0)}_m$ is determined by Eq. (54), and Eq. (55) gives that

$$u^{(0)}_{m-1/2} = u^{(0)}_{m+1/2} \equiv \bar{u}^{(0)}_m. \tag{56}$$

Away from the extremum, the node values $u^{(0)}_{k-1/2}$, for $k < m$ and $k > m + 1$, are governed by Eq. (29). In words, Eq. (54) applies in the cell containing the extremum, with its surrounding node values given by Eq. (56). For all other nodes, Eq. (29) holds. Eqs. (54) and (29) are both second-order accurate discretizations of the heat equation, although Eq. (56) is a first-order interpolant in space. How this local error analysis manifests itself into the global error is left for future work. The convergence rate can be no worse than first order. But our numerical results in Section 6 will demonstrate that the numerical solution converges at roughly a second-order rate to the asymptotic solution.

Away from the asymptotic limit, in general, a slope limiter might adjust the slope in the cells on either side of the cell with the extremum. However, in the asymptotic limit, this is no longer the case. When the cell at an extreme point is slope limited, the neighboring cells will still have continuous cell edge values (guaranteed by the solvability condition). This continuity of the discrete solution, coupled with Eq. (56), means that double minmod will not affect the neighboring cells. Our numerical results will demonstrate that cells away from the extreme point are not affected.

The final possibility is that the extremum occurs exactly at the interface between two cells. Let the corresponding cell indices be m and $m + 1$. Any limiter of the form (33) will zero the slope in both of these cells. But it is easy to show that the quantity

$$\tilde{u}^{(0)}_{m+1/2} = \frac{1}{2}(\bar{u}^{(0)}_m + \bar{u}^{(0)}_{m+1}) \tag{57}$$

satisfies the discretization of the form (29). Also, following similar arguments as above,

$$u^{(0)}_{m-1/2} = u^{(0)}_{m+1/2} = u^{(0)}_{m+3/2} \equiv \tilde{u}^{(0)}_{m+1/2} \tag{58}$$

and away from the extremum, the node values $u^{(0)}_{k-1/2}$, $k < m$ and $k > m+2$, are governed by Eq. (29). Similar to the case where the slope is limited only in a single cell, the evolution equations are second-order accurate in space, but the interpolant (58) is locally only first-order accurate.

5. Sawtooth-free limiter

The double minmod method will preserve the asymptotic limit for the hyperbolic heat equation. One issue with this limiter is that it allows false extrema, or "sawteeth", in the solution when the cell-edge values are plotted. Though the double minmod limiter gives a method that is total variation diminishing in the means [15], in strongly nonlinear problems or problems where the cell-edge values feed into another physical operator these sawteeth can lead to a lack of robustness in engineering calculations. In order to eliminate the sawteeth, in this section we seek a more diffusive limiter that still maintains the proper asymptotic limit.

A sawtooth at the edge between cell m and $m+1$ is defined as when the slope in both cells have the same sign:

$$(u_{m,2} - u_{m,1})(u_{m+1,2} - u_{m+1,1}) > 0, \tag{59a}$$

but the difference at the cell edge has a different sign than the slope:

$$(u_{m,2} - u_{m,1})(u_{m+1,2} - u_{m,2}) < 0. \tag{59b}$$

We can eliminate these sawteeth with an approach that is very similar to the removal of false extrema by Liu and Osher [18].

Our method begins with an application of the double minmod limiter, to give limited values that we will refer to in this section as $u_{m,j}$. We then perform a cell-by-cell check for sawteeth. In cell m we check each edge for a sawtooth using the conditions (59). If only one side has a sawtooth, for example the interface of $u_{m,2}$ and $u_{m+1,1}$, it is removed by the following procedure. First, we compute a desired face value, u_{face}:

$$u_{\text{face}} = \frac{u_{m,2} + u_{m+1,1}}{2} \tag{60}$$

and then define a new slope for cell m and $m+1$:

$$\tilde{s}_m = 2(u_{\text{face}} - \bar{u}_m), \tag{61}$$

$$\tilde{s}_{m+1} = 2(\bar{u}_{m+1} - u_{\text{face}}). \tag{62}$$

Using these slopes we compute new values at the nodes in the cell:

$$\tilde{u}_{m,1} = \bar{u}_m - \frac{1}{2}\tilde{s}_m, \qquad \tilde{u}_{m,2} = \bar{u}_m + \frac{1}{2}\tilde{s}_m. \tag{63}$$

If both sides of the cell have a sawtooth, we then compute the difference between nodes on each side:

$$\Delta_{m+1/2} = u_{m+1,1} - u_{m,2}, \tag{64}$$

$$\Delta_{m-1/2} = u_{m,1} - u_{m-1,2}. \tag{65}$$

Whichever edge has a Δ of a larger magnitude, on that side we correct that edge as though it were the only sawtooth.

This procedure has the effect of, in the case of a sawtooth on both sides of the cell, making the edge with a smaller sawtooth a jump. To see this we look at the example of $|\Delta_{m+1/2}| > |\Delta_{m-1/2}|$ and an increasing function. If we assume that the $m-1$ has only one sawtooth, then

$$\tilde{u}_{m-1,2} = \frac{1}{2}(u_{m,1} + u_{m-1,2}). \tag{66}$$

The value of the left edge of cell m will be

$$\tilde{u}_{m,1} = \bar{u}_m - \frac{1}{2}\tilde{s}_m = \frac{1}{2}(2u_{m,1} - \Delta_{m+1/2}). \tag{67}$$

Because we are dealing with the case where s_m is positive, $\Delta_{m+1/2}$ is negative and $\Delta_{m-1/2}$ is negative but of a lesser magnitude. This implies that

$$\tilde{u}_{m,1} > \bar{u}_m - \frac{1}{2}\tilde{s}_m = \frac{1}{2}(2u_{m,1} - \Delta_{m-1/2}) = \frac{1}{2}(u_{m,1} + u_{m-1,2}) = \tilde{u}_{m-1,2}. \tag{68}$$

Therefore, there will be a jump at left edge of cell m instead of a sawtooth.

We now will show that our procedure from removing sawteeth does not increase the value of $|s_m|$. To illustrate this we will assume that we are removing the sawtooth at the right edge of the cell; however, our treatment trivially generalizes to a sawtooth on the left edge. The value of s_m after the initial pass of the double minmod limiter is $u_{m,2} - u_{m,1}$ and $s_{m+1} = u_{m+1,2} - u_{m+1,1}$. We note that when these initial slopes s_m and s_{m+1} are positive, that

$$u_{m+1,1} \leqslant u_{\text{face}} \leqslant u_{m,2}. \tag{69}$$

In this case then

$$\tilde{s}_m \leqslant (u_{m,2} - u_{m,1}) = s_m. \tag{70}$$

The same argument holds for the case of s_m and s_{m+1} both negative. In this case

$$u_{m,2} \leqslant u_{\text{face}} \leqslant u_{m+1,1}. \tag{71}$$

This leads to

$$s_m \geqslant 2(\bar{u}_m - u_{\text{face}}) = \tilde{s}_m. \tag{72}$$

Hence, our step to remove sawteeth will not increase the magnitude of the slope.

Finally, our implementation of this procedure stores the ũ's separately so that the limited results are independent of the order in which cells are visited.

6. Numerical results

We will now demonstrate the conclusions of our analysis with numerical results. In these results the time integration method used is the predictor corrector method given in Section 2 and we will define the CFL number as CFL = $c\Delta t/\Delta x$.

Consider an infinite medium and the following initial condition:

$$u(x,0) = v(x,0) = H(x-1)H(2-x), \tag{73}$$

where $H(x)$ is the Heaviside step function.

The exact solution to Eq. (16) for this problem is

$$u(x,t) = \frac{1}{2}\left[\text{Erf}\left(\frac{x-1}{2\sqrt{\tau t}}\right) - \text{Erf}\left(\frac{x-2}{2\sqrt{\tau t}}\right)\right], \tag{74}$$

where Erf(z) is the error function.

Figs. 1 and 2 show the effects of different limiters for this problem. The numerical solutions were obtained using a large enough domain so that information from the initial condition never made it to the simulation boundary. With $\tau = 10^{-2}$ the step method is already unacceptably inaccurate, as shown in Fig. 1. In this case, $h = 200$, and thus the problem is moderately stiff. Although the minmod limiter performs better than step, it does not capture the exact solution. The double minmod limiter captures the asymptotic solution quite well. The sawtooth-free limiter results are slightly different than the double minmod results. This discrepancy arises from the fact that the initial condition is not a diffusion solution, which induces a numerical initial layer. This initial layer is not symmetric about $x = 1.5$ because $v(x,0) \neq 0$ introduces directionality into the initial layer. In the first time step the double minmod limiter produces sawteeth, one on each side of the square wave, and the sawtooth-free limiter removes these. Despite this different treatment early in the problem, both the double minmod and sawtooth-free limiters capture the asymptotic solution.

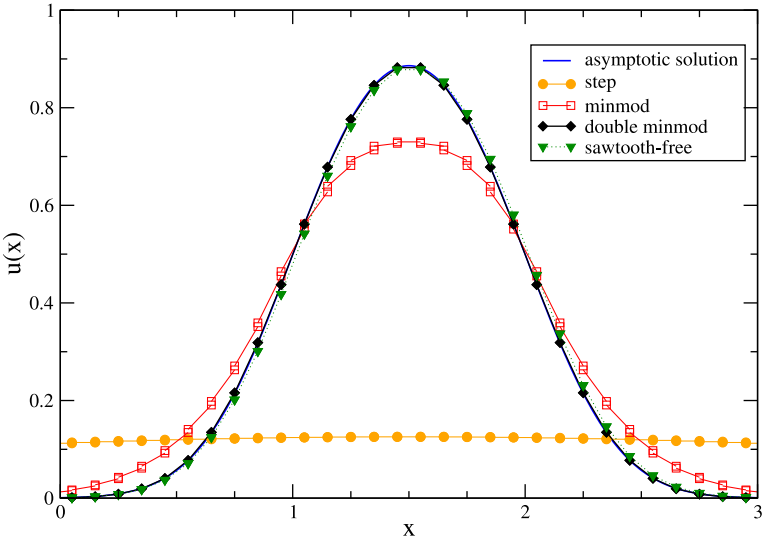

Fig. 1. Comparison of different slope limiters with an exact solution to the asymptotic limit equations with a square initial condition and $\tau = 10^{-2}$ at $t = 5$. The numerical solutions used: $\Delta x = 0.1$ and CFL = 0.3.

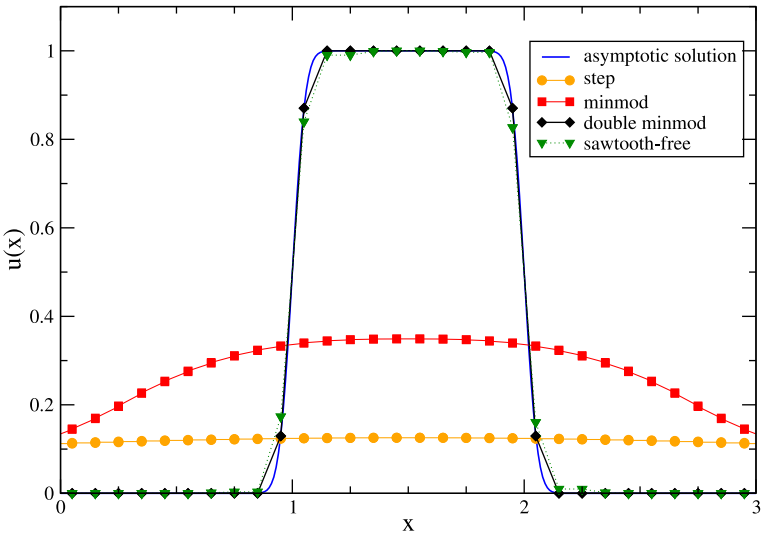

Fig. 2. The results from different limiters on a stiffer version of the problem ($\tau = 10^{-5}$) from Fig. 1 at $t = 100$. The numerical solutions used: $\Delta x = 0.1$ and CFL = 0.3.

In the stiffer version of this problem ($h = 2 \times 10^4$) shown in Fig. 2, only the double minmod and sawtooth-free limiters give a reasonable solution. In this problem the differences between the sawtooth-free and double minmod limiters can be readily seen in the edges of the square wave.

To demonstrate the need for the sawtooth-free limiter we also solve a problem without significant relaxation terms. Figs. 3 and 4 give a solution to the square wave problem defined above but with $\tau = 10^{10}$. In these figures the hyperbolic solution to this problem and the diffusion solution are shown. In this problem we would expect our numerical method to approximate the hyperbolic solution because the relaxation terms are so small. The results show that the double minmod limiter performs the best in capturing the shape of the solution. However, the sawteeth in the double minmod solution are apparent. The sawtooth-free limiter does remove the sawteeth while sacrificing a small amount of accuracy. Despite being less accurate than double minmod, the sawtooth-free limiter performs better than the minmod limiter.

The next problem we will look at has an initial condition of

$$u(x,0) = 3\sin\left(\frac{\pi x}{3}\right) + 3, \qquad v(x,0) = 0 \tag{75}$$

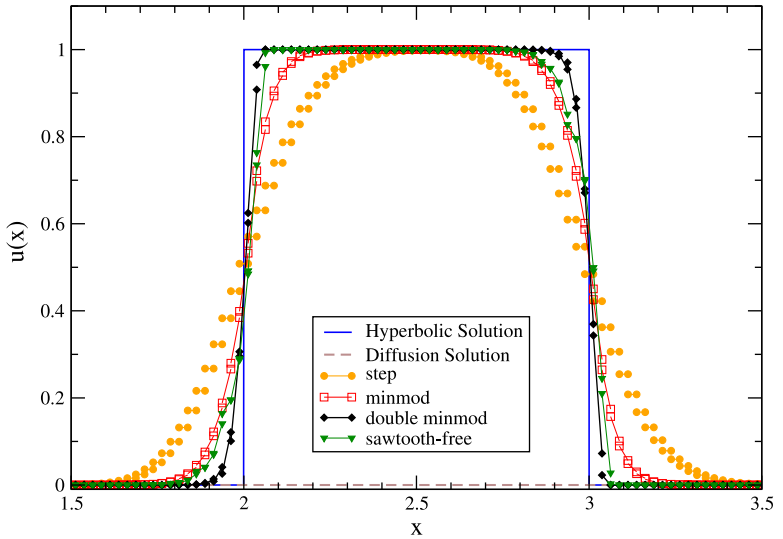

Fig. 3. Solutions from the square wave problem with $\tau = 10^{10}$ at $t = 1$. In this problem the relaxation terms are negligible. The numerical solutions used: $\Delta x = 0.025$ and CFL = 0.3.

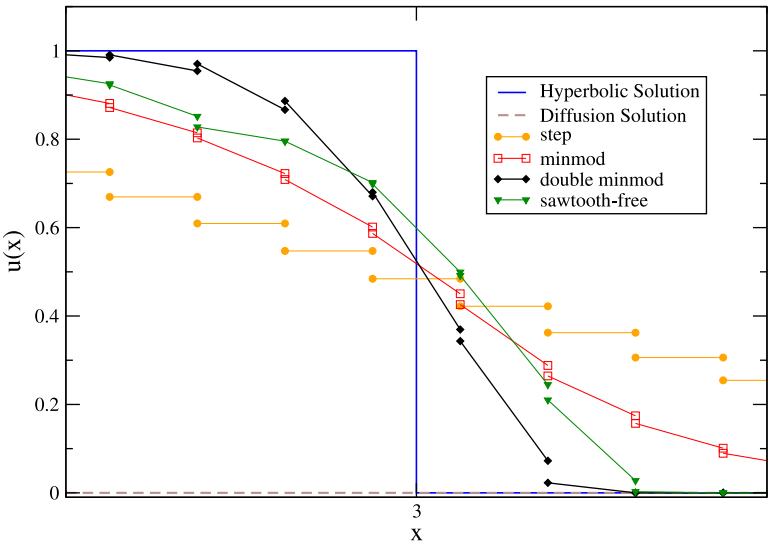

Fig. 4. Detail of Fig. 3.

and periodic boundary conditions. The exact solution to the heat equation for this initial condition is

$$u(x,t) = 3 + 3e^{-\frac{\pi^2}{9}\tau t}\sin\left(\frac{\pi x}{3}\right). \tag{76}$$

The solution to this problem will have clipping at the extrema of the sine wave, and results for this situation will further explore the behavior at extreme points. Fig. 5 shows the behavior of the error with mesh refinement. Here, a sine wave initial condition is used, $\tau = 10^{-4}$, and the errors are computed at $t = 500$. In Fig. 5, the error is measured in the L_∞ norm of the nodal values:

$$L_\infty(u_{\text{asymptotic}}(x,t) - u_{\text{numerical}}(x,t)) = \max_{m=1,\ldots,N_x} |u_{\text{asymptotic}}(x_m,t) - u_{\text{numerical}}(x_m,t)|. \tag{77}$$

Here, N_x is the number of node values. The results show that errors from the double minmod and sawtooth-free methods decay at a second-order rate, despite the clipping of extrema. This convergence study has every value of $\Delta x \gg \tau$, and therefore, tests the convergence in the asymptotic limit. The step and minmod limiters show no convergence when the relaxation term is totally unresolved. The error using the minmod limiter does not begin to decrease until $\Delta x \leqslant 0.1$; the step limiter's

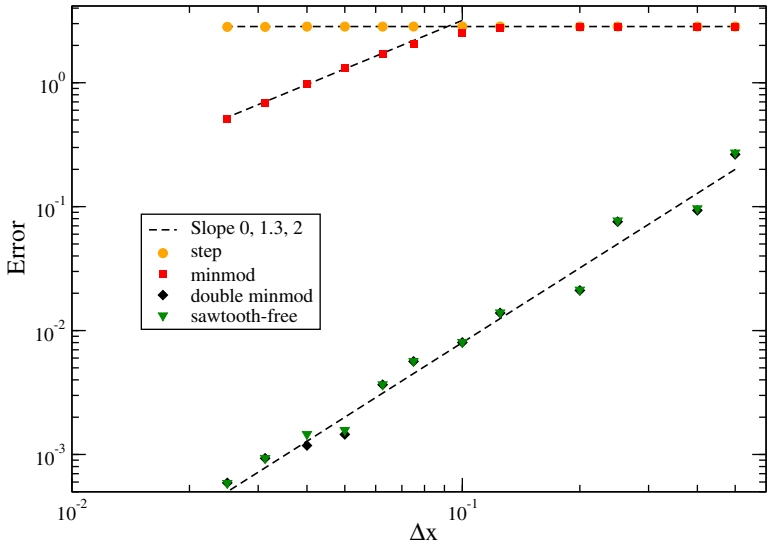

Fig. 5. The L_∞ error for the sine wave problem with $\tau = 10^{-4}$ and CFL = 0.3 at $t = 500$.

error is constant. Once the minmod limiter does begin to converge it does so at $O(\Delta x^{1.3})$. The smallest error in the minmod solution was no better than the highest error in the solutions with the double minmod or sawtooth-free limiters.

6.1. Advection–diffusion results

If the second equation in the hyperbolic heat system, Eq. (13), is modified to

$$\frac{\partial v}{\partial t}+\frac{\partial u}{\partial x}=\frac{1}{\tau}(au-v),\quad 0<a^2<1. \tag{78}$$

The asymptotic limit of the system becomes [13]

$$\frac{\partial u}{\partial t}+a\frac{\partial u}{\partial x}=\tau(1-a^2)\frac{\partial^2 u}{\partial x^2}. \tag{79}$$

Whereas the asymptotic limit in the case of $a = 0$ was a diffusion equation, Eq. (16), the limit when $a \neq 0$ has a streaming term. Therefore, a numerical method for Eq. (79) will require a slope limiter in the asymptotic limit. A slope limiter will become more important when the streaming term dominates the diffusion term.

We can quantify the amount of streaming compared with relaxation by defining a Peclet number for this equation [13]

$$Pe=\frac{a}{\tau(1-a^2)}. \tag{80}$$

For large values of Pe the asymptotic limit will be dominated by the streaming term; $Pe \to 0$ causes the diffusive term to dominate.

This advection–diffusion limit was examined by Lowrie and Morel [13] for the DG method without a slope limiter. They showed that the DG method was asymptotic preserving for any Peclet number. Here we will see that the slope limiter affects this property of the DG method.

We will apply the different slope limiters to the modified problem with $a \neq 0$. The initial condition is Eq. (75), and in this case the solution is

$$u(x,t)=3+3e^{\frac{\pi^2}{9}(a^2-1)\tau t}\sin\left(\frac{\pi}{3}(x-at)\right). \tag{81}$$

The error convergence for this problem are shown in Fig. 6. Each simulation was run until the initial condition propagated one wavelength.

For a Peclet number of 100, the double-minmod and sawtooth-free limiters converged to the analytic solution at second order. When the Peclet number was 10^6 (a problem that is dominated by advection), the double-minmod and sawtooth-free limiters converged at a rate of $O(\Delta x^{1.6})$. We observed the same convergence rate when the double minmod limiter was applied to a linear advection problem with a sinusoidal solution. For this high Peclet number the sawtooth-free limiter performed slightly better than the double minmod limiter. This is due to the fact that because advection dominates in this

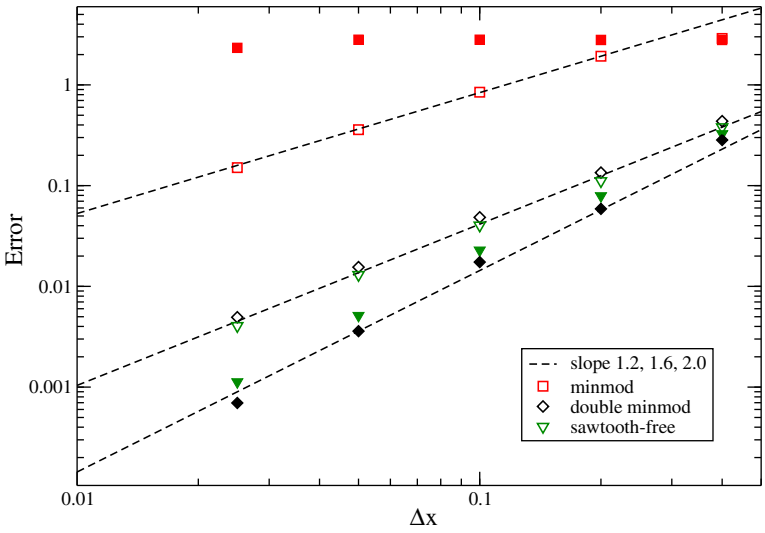

Fig. 6. The L_∞ error for the case of advection and diffusion with $\tau = 10^{-4}$ and CFL = 0.3. The solid symbols have $Pe = 100$ while the outlined symbols have $Pe = 10^6$.

problem, sawteeth do develop and affect the L_∞ norm of the error. The sawtooth-free limiter improves the solution error by removing these sawteeth.

At *Pe = 100* the minmod limiter did not converge, whereas, at the high Peclet number the method converged at a rate of $O(\Delta x^{1.2})$. The discrepancy between convergence rates at low versus high Peclet numbers for the minmod method is analogous to the behavior of the Liotta, Romano and Russo method (LRR) [19]. The LRR method, like the minmod limited discontinuous Galerkin method, is convergent for large Peclet numbers, but does not converge for small Peclet numbers when the relaxation terms are not resolved [13].

7. Thermal radiation transport equations

We will now extend our analysis of the hyperbolic heat equation to the more complicated case of thermal radiation transport. This system has nonlinear relaxation terms. For a discrete version of this system our results from the hyperbolic heat analysis will carry over.

The equations of thermal radiation transport are governed by an infinite-dimensional hyperbolic system of equations coupled to an equation that models the internal energy of the background material. The grey intensity of radiation, $I(x,\mu,t)$, in plane-parallel geometry is given by [20]

$$\frac{1}{c}\frac{\partial I}{\partial t}+\mu\frac{\partial I}{\partial x}+\sigma I=\frac{1}{2}\sigma acT^4, \tag{82}$$

where $\mu\in[-1,1]$ is the direction-of-flight or angular variable, $\sigma(x,t)$ is the absorption opacity, a is the radiation constant and $T(x,t)$ is the temperature of the material the radiation is transporting through. The material temperature is governed by

$$\frac{\partial e}{\partial t}=\int_{-1}^{1}\mathrm{d}\mu\sigma\left(I-\frac{1}{2}acT^4\right) \tag{83}$$

with $e(x,t,\rho,T)$ internal energy. The internal energy is related to the temperature through an equation of state. When the background material is stationary we can write

$$\frac{\partial e}{\partial t}=\frac{\partial e}{\partial T}\frac{\partial T}{\partial t}=C_v\frac{\partial T}{\partial t}. \tag{84}$$

C_v is the heat capacity of the material.

The thermal radiation transport system asymptotically limits to a nonlinear diffusion equation. This is derived by making the opacity large and the temporal variations small using a small, positive, parameter ϵ [21] to get

$$\epsilon\frac{1}{c}\frac{\partial I}{\partial t}+\mu\frac{\partial I}{\partial x}+\frac{\sigma}{\epsilon}I=\frac{1}{2\epsilon}\sigma acT^4, \tag{85}$$

$$\epsilon\frac{\partial e}{\partial t}=\int_{-1}^{1}\mathrm{d}\mu\frac{\sigma}{\epsilon}\left(I-\frac{1}{2}acT^4\right). \tag{86}$$

In the limit of small ϵ the leading order the intensity is in equilibrium with the blackbody source

$$I=\frac{1}{2}acT^4 \tag{87}$$

and the leading-order temperature is governed by

$$\frac{\partial e}{\partial t}+a\frac{\partial T^4}{\partial t}=ac\frac{\partial}{\partial x}\frac{1}{3\sigma}\frac{\partial T^4}{\partial x}. \tag{88}$$

7.1. P_N equations

The radiation transport system is continuous in μ as well as x and t. There are various ways of treating the direction-of-flight variable, and the one we will discuss is the spherical harmonics (P_N) method. In one-dimensional problems this approach expands μ in Legendre polynomials. The expansion is truncated at some level n. Eqs. (82) and (83) become [22,23]

$$\frac{1}{c}\frac{\partial I_0}{\partial t}+\frac{\partial I_1}{\partial x}+\sigma I_0=\sigma acT^4,\quad l=0, \tag{89a}$$

$$\frac{1}{c}\frac{\partial I_l}{\partial t}+\frac{l}{2l+1}\frac{\partial I_{l-1}}{\partial x}+\frac{l+2}{2l+1}\frac{\partial I_{l+1}}{\partial x}+\sigma I_l=0,\quad 1\leqslant l\leqslant n. \tag{89b}$$

The moments of the intensity, I_l, are defined by

$$I_l=\int_{-1}^{1}P_l(\mu)I(\mu)\,\mathrm{d}\mu, \tag{90}$$

where P_l is the lth Legendre polynomial. To close the system, I_{n+1} is set to zero. The material energy equation only involves the zeroth moment of I:

$$\frac{\partial e}{\partial t} = \sigma\left(I_0 - acT^4\right). \tag{91}$$

We use the same time integration as described in Section 2. The time integration for the P_N equations is different from the hyperbolic heat equation because of the nonlinearities arising from the T^4 terms. We use a linearization based on a first-order Taylor expansion of T^4; see Refs. [24,25] for details.

McClarren et al. [24] showed that the asymptotic limit of the DG method for the P_N equations gives a valid discretization of Eq. (88) and enforces the equilibrium of Eq. (87).

The analysis that leads to this discrete diffusion equation hinges on the fact that in the limit of small ϵ, I_0 is continuous on a cell edge. In this respect, the asymptotic analysis is similar to that for the hyperbolic heat equation presented earlier. In their study, McClarren et al. did not consider the effects of a slope limiter on the diffusion limit. A slope limiter that breaks continuity will modify these equations and give a different leading-order equation for I_0 as in our analysis of the hyperbolic heat equation. Though a slope limiter can break the diffusion limit, it will not harm the equilibrium between the blackbody source and I_0.

As in the hyperbolic heat equation, the method will make the cell-averages equal,

$$\bar{I}^{(0)}_{0,m+1} = \bar{I}^{(0)}_{0,m}, \tag{92}$$

and the minmod limiter will give that the second derivative of the leading-order solution will be of order Δx:

$$\frac{\partial^2 I^{(0)}_0}{\partial x^2} = \mathrm{O}(\Delta x). \tag{93}$$

Both step and minmod will give the incorrect evolution equation as derived for the hyperbolic heat case.

The double minmod limiter (and the sawtooth-free version of this limiter) will not corrupt the continuity of I_0 and will lead to a correct diffusion discretization.

7.2. Numerical results

A common problem with stiff temperature feedback is the Marshak wave problem in a highly absorptive medium. This problem has an initial cold semi-infinite medium with a 1 keV temperature source at $x = 0$. The material has $\sigma = 300/T^3$ where the units of σ are cm^{-1} and T is in keV along with $C_v = 0.3 \times 10^{16}$ erg/cm^3/keV. In this problem the diffusion solution will agree with the transport solution because the background material is so optically thick that transport effects are negligible. There is a semi-analytic diffusion solution to this problem that we will compare numerical results to. For our numerical solution we will use an initial condition of $T(x,0) = 10^{-9}$ keV and $I(x,0) = 1/2ac(T(x,0))^4$.

The numerical solutions in Figs. 7 and 8 show the necessity of having a limiter that preserves the continuity of the numerical solution. In these results h ($h = \sigma\Delta x$ in radiation problems) ranges from 11 in the warm region of the problem to 10^{28} in

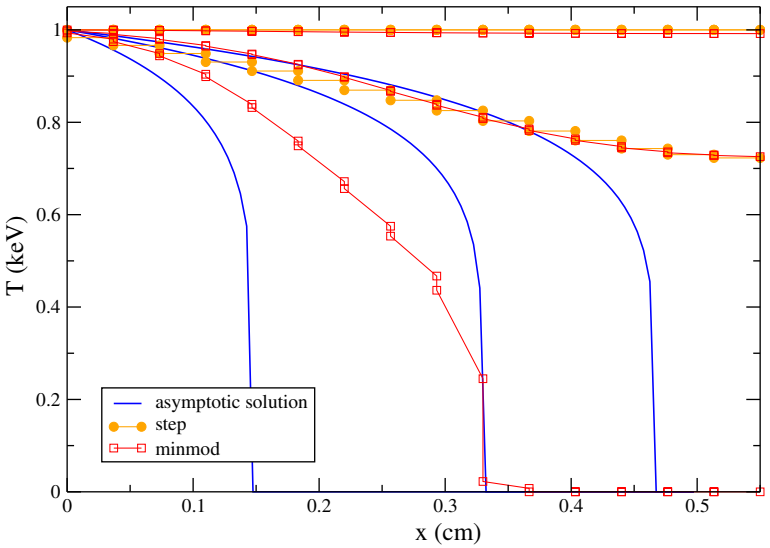

Fig. 7. The solution for the material temperature from the step and minmod limiters compared with the semi-analytic solution to the Marshak wave problem. The solutions are at $t = 10$, 50, 100 ns. The step method numerical solutions at 0.5 and 1.0 ns solutions are coincident at the top of the figure. The numerical solutions used: $\Delta x = 0.0366$ cm and $\Delta t = 5 \times 10^{-3}$ ns.

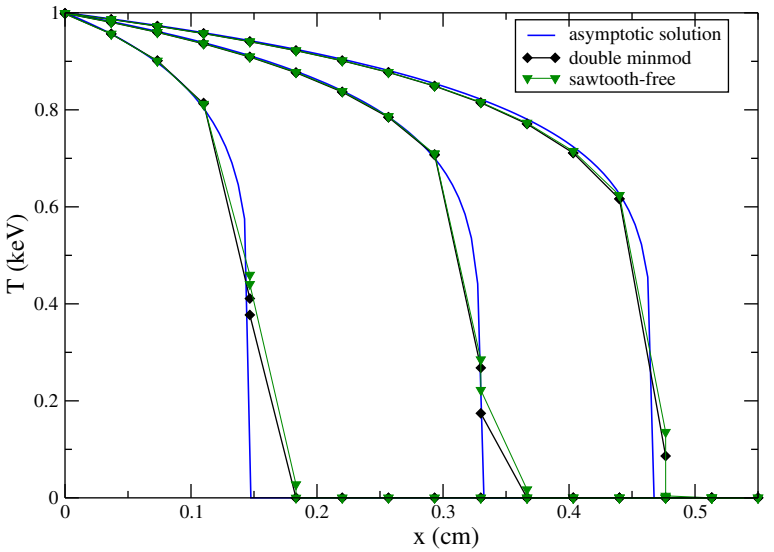

Fig. 8. The material temperature from the double minmod and sawtooth-free limiters for the Marshak wave problem at $t = 10, 50, 100$ ns. The numerical solutions used: $\Delta x = 0.0366$ cm and $\Delta t = 5 \times 10^{-3}$ ns.

the cold regions. Fig. 7 demonstrates that the step method gives a nearly flat solution as predicted by our analysis. The minmod limiter performs better than step, but near the sharp wavefront the limiter forces the solution to have a negligible second derivative. This is especially clear in the 10 ns solution where the wavefront is warped into a linear curve. The double minmod limiter, as predicted, captures the diffusion solution as well as possible using a coarse grid. The sawtooth-free limiter also captures the diffusion solution, but is different than the double minmod answer at the edge of the wavefront. The wavefront is non-smooth and not even double minmod can remain continuous in this region of the problem. This allows the creation of sawteeth leading to the difference between the double minmod solutions and the sawtooth-free results. Despite the differences at the wavefront, the sawtooth-free and double minmod solutions agree well in the smooth regions of the solution.

8. Conclusions

In this study, we have shown that in order to preserve the asymptotic behavior of the DG method, a slope limiter should not introduce discontinuities at the cell edge. The minmod limiter introduces discontinuities and thus fails to preserve the asymptotic limit. We showed that the double minmod limiter is asymptotic preserving, along with a "sawtooth-free" limiter that we introduced. The sawtooth-free limiter is more diffusive than double minmod, but should also be more robust for highly nonlinear systems. Our analysis was applied to the hyperbolic heat equation and the thermal P_N equations and numerical results backed up the results of our analysis. Future work should apply these limiters to more complex systems. In more complex cases, it may be necessary to avoid clipping of smooth extrema, such as by using the smoothness detector of Ref. [15].

References

[1] R.B. Lowrie, J.E. Morel, Discontinuous Galerkin for hyperbolic systems with stiff relaxation, in: B. Cockburn, G.E. Karniadakis (Eds.), Discontinuous Galerkin Methods: Theory, Computation and Applications, Springer, Berlin, 2000, pp. 385–390.
[2] R.B. Lowrie, J.E. Morel, Issues with high-resolution Godunov methods for radiation hydrodynamics, J. Quant. Spectr. Radiat. Transfer 69 (2001) 475–489.
[3] E.W. Larsen, The asymptotic diffusion limit of discretized transport problems, Nucl. Sci. Eng. 112 (1992) 336–346.
[4] E.W. Larsen, J.B. Keller, Asymptotic solution of neutron transport problems for small mean free paths, J. Math. Phys. 15 (1) (1974) 75–81.
[5] S. Harris, Introduction to the Theory of the Boltzmann Equation, Dover Publications, New York, 1971.
[6] S. Jin, C.D. Levermore, Numerical schemes for hyperbolic conservation laws with stiff relaxation terms, J. Comp. Phys. 126 (1996) 449–467.
[7] S. Jin, Efficient asymptotic-preserving (ap) schemes for some multiscale kinetic equations, SIAM J. Sci. Comp. 21 (1999) 441–454.
[8] E.W. Larsen, J.E. Morel, W.F. Miller, Asymptotic solutions of numerical transport problems in optically thick, diffusive regimes, J. Comp. Phys. 69 (2) (1987) 283–324.
[9] J.D. Densmore, E.W. Larsen, Asymptotic equilibrium diffusion analysis of time-dependent Monte Carlo methods for grey radiative transfer, J. Comp. Phys. 199 (2004) 175–204.
[10] J.E. Morel, T.A. Wareing, K. Smith, A linear-discontinuous spatial differencing scheme for S_n radiative transfer calculations, J. Comp. Phys. 128 (1996) 445–462.
[11] M.L. Adams, Discontinuous finite element transport solutions in thick diffusive problems, Nucl. Sci. Eng. 137 (2001) 298–333.
[12] E.W. Larsen, J.E. Morel, Asymptotic solutions of numerical transport problems in optically thick, diffusive regimes II, J. Comp. Phys. 83 (1989) 212–236.

[13] R.B. Lowrie, J.E. Morel, Methods for hyperbolic systems with stiff relaxation, Int. J. Numer. Method Fluids 40 (2002) 413–423.
[14] B. Cockburn, C. Shu, The Runge–Kutta local projection P^1-discontinuous-Galerkin finite element method for scalar conservation laws, ESAIM: Math. Model. Numer. Anal. (M^2AN) 25 (1991) 337–361.
[15] B. Cockburn, C. Shu, TVB Runge–Kutta projection discontinuous Galerkin finite element method for conservation laws II: General framework, Math. Comput. 52 (186) (1989) 411–435.
[16] B. van Leer, Towards the ultimate conservative difference scheme IV. A new approach to numerical convection, J. Comp. Phys. 23 (3) (1977) 276–299.
[17] R.G. McClarren, J.P. Holloway, T.A. Brunner, T.A. Mehlhorn, A quasi-linear implicit Riemann solver for the time-dependent P_n equations, Nucl. Sci. Eng. 155 (2007) 290–299.
[18] X.-D. Liu, S. Osher, Nonoscillatory high order accurate self-similar maximum principle satisfying shock capturing schemes. I, SIAM J. Numer. Anal. 33 (2) (1996) 760–779.
[19] S.F. Liotta, V. Romano, G. Russo, Central schemes for balance laws of relaxation type, SIAM J. Numer. Anal. 38 (2000) 1337–1356.
[20] G.C. Pomraning, The Equations of Radiation Hydrodynamics, Pergamon Press, Oxford, 1973.
[21] E.W. Larsen, G.C. Pomraning, V.C. Badham, Asymptotic analysis of radiative transfer problems, J. Quant. Spectr. Radiat. Transfer 29 (4) 285–310.
[22] G.I. Bell, S. Glasstone, Nuclear Reactor Theory, Robert E. Kreiger Publishing, Malabar, FL, 1970.
[23] R.G. McClarren, J.P. Holloway, T.A. Brunner, An implicit P_n method for thermal radiative transfer, J. Comp. Phys. 227 (2008) 2864–2885.
[24] R.G. McClarren, T.M. Evans, R.B. Lowrie, J.D. Densmore, Semi-implicit time integration for P_N thermal radiative transfer, J. Comp. Phys. 227 (2008) 7561–7586.
[25] J.A. Fleck Jr., J.D. Cummings, An implicit Monte Carlo scheme for calculating time and frequency dependent nonlinear radiation transport, J. Comp. Phys. 8 (1971) 313–342.